

# Reachability-Based Safety and Goal Satisfaction of Unmanned Aerial Platoons on Air Highways

Mo Chen,\* Qie Hu,\* Jaime F. Fisac,\* Kene Akametalu,\* Casey Mackin,† and Claire J. Tomlin‡  
*University of California, Berkeley, Berkeley, California 94720-1770*

DOI: 10.2514/1.G000774

Recently, there has been immense interest in using unmanned aerial vehicles for civilian operations. As a result, unmanned aerial systems traffic management is needed to ensure the safety and goal satisfaction of potentially thousands of unmanned aerial vehicles flying simultaneously. Currently, the analysis of large multi-agent systems cannot tractably provide these guarantees if the agents' set of maneuvers is unrestricted. In this paper, platoons of unmanned aerial vehicles flying on air highways is proposed to impose an airspace structure that allows for tractable analysis. For the air highway placement problem, the fast marching method is used to produce a sequence of air highways that minimizes the cost of flying from an origin to any destination. The placement of air highways can be updated in real time to accommodate sudden airspace changes. Within platoons traveling on air highways, each vehicle is modeled as a hybrid system. Using Hamilton–Jacobi reachability, safety and goal satisfaction are guaranteed for all mode transitions. For a single altitude range, the proposed approach guarantees safety for one safety breach per vehicle; in the unlikely event of multiple safety breaches, safety can be guaranteed over multiple altitude ranges. This paper demonstrates the platooning concept through simulations of three representative scenarios.

## Nomenclature

$C$	=	cumulative cost of a path
$c$	=	cost map
$\hat{d}$	=	direction of travel of air highway
$d_{\text{sep}}$	=	separation distance of vehicles within a platoon
$\mathcal{H}$	=	air highway
$\mathcal{P}$	=	path between two points
$p$	=	$(p_x, p_y)$ , horizontal position
$\bar{p}$	=	target position
$Q_i$	=	$i$ th vehicle
$\mathcal{Q}_i$	=	set of vehicles for vehicle $Q_i$ to consider for safety
$\mathcal{S}$	=	sequence of air highways
$t_{\text{faulty}}$	=	time limit for descent during potential conflict
$V$	=	value function of partial differential equations
$v$	=	$(v_x, v_y)$ , horizontal velocity
$\bar{v}$	=	target velocity
$\mathcal{W}$	=	waypoint
$x$	=	system state (of a vehicle)

## I. Introduction

UNMANNED aerial vehicles (UAVs) have in the past been mainly used for military operations [1]; however, recently there has been an immense surge of interest in using UAVs for civil applications. Through projects such as Amazon Prime Air<sup>8</sup> and Google Project Wing [2], companies are looking to send UAVs into the airspace to not only deliver commercial packages, but also for important tasks such as aerial surveillance, emergency supply delivery, videography, and search and rescue [3]. In the future, the use of UAVs is likely to become more and more prevalent.

Received 15 July 2016; revision received 17 November 2016; accepted for publication 18 November 2016; published online 30 January 2017. Copyright © 2016 by the American Institute of Aeronautics and Astronautics, Inc. All rights reserved. All requests for copying and permission to reprint should be submitted to CCC at [www.copyright.com](http://www.copyright.com); employ the ISSN 0731-5090 (print) or 1533-3884 (online) to initiate your request. See also AIAA Rights and Permissions [www.aiaa.org/randp](http://www.aiaa.org/randp).

\*Ph.D. Candidate, Department of Electrical Engineering and Computer Sciences.

†Ph.D. Student, Department of Electrical Engineering and Computer Sciences.

‡Professor, Department of Electrical Engineering and Computer Sciences. Member AIAA.

<sup>8</sup>Data available online at <http://www.amazon.com/b?node=8037720011> [retrieved 17 October 2016].

As a rough estimate, suppose in a city of 2 million people, each person requests a drone delivery every two months on average and each delivery requires a 30 min trip for a UAV. This would equate to thousands of UAVs simultaneously in the air just from package delivery services. Applications of UAVs extend beyond package delivery; they can also be used, for example, to provide supplies or to respond to disasters in areas that are difficult to reach but require prompt response [4,5]. As a result, government agencies such as the Federal Aviation Administration and NASA are also investigating unmanned aerial systems (UASs) traffic management to prevent collisions among potentially numerous UAVs [3,6,7].

Optimal control and game theory present powerful tools for providing safety and goal satisfaction guarantees to controlled dynamical systems under bounded disturbances, and various formulations [8–10] have been successfully used to analyze problems involving small numbers of vehicles [11–14]. These formulations are based on Hamilton–Jacobi (HJ) reachability, which can compute the backward reachable set (BRS), defined as the set of states from which a system is guaranteed to have a control strategy to reach a target set of states. HJ reachability is a powerful tool because BRS can be used for synthesizing both controllers that steer the system away from a set of unsafe states (“safety controllers”) to guarantee safety and controllers that steer the system into a set of goal states (“goal satisfaction controllers”) to guarantee goal satisfaction. Unlike many formulations of reachability, the HJ formulations are flexible in terms of system dynamics, enabling the analysis of controlled nonlinear systems under disturbances. Furthermore, HJ reachability analysis is complemented by many numerical tools readily available to solve the associated HJ partial differential equation (PDE) [15–17]. However, the computation is done on a grid, making the problem complexity scale exponentially with the number of states and therefore with the number of vehicles. Consequently, HJ reachability computations are intractable for large numbers of vehicles.

To accommodate potentially thousands of vehicles simultaneously flying in the air, additional structure is needed to allow for tractable analysis and intuitive monitoring by human beings. An air highway system on which platoons of vehicles travel accomplishes both goals. However, many details of such a concept need to be addressed. Because of the flexibility of placing air highways compared with building ground highways in terms of highway location, even the problem of air highway placement can be a daunting task. To address this, in the first part of this paper, we propose a flexible and computationally efficient method based on [17] to perform optimal air highway placement given an arbitrary cost map that captures the desirability of having UAVs fly over any geographical location. We

demonstrate our method using the San Francisco Bay Area as an example. Once air highways are in place, platoons of UAVs can then fly in fixed formations along the highway to get from origin to destination. The air highway structure greatly simplifies safety analysis, while at the same time allows intuitive human participation in unmanned airspace management.

A considerable body of work has been done on the platooning of ground vehicles [18]. For example, McMahon et al. [19] investigated the feasibility of vehicle platooning in terms of tracking errors in the presence of disturbances, taking into account complex nonlinear dynamics of each vehicle. Hedrick et al. [20] explored several control techniques for performing various platoon maneuvers, such as lane changes, merge procedures, and split procedures. In [21], the authors modeled vehicles in platoons as hybrid systems, synthesized safety controllers, and analyzed throughput. Reachability analysis was used in [22] to analyze a platoon of two trucks to minimize drag by minimizing the following distance while maintaining collision avoidance safety guarantees. Finally, Sabau et al. [23] provided a method for guaranteeing string stability and eliminating accordion effects for a heterogeneous platoon of vehicles with linear time-invariant dynamics.

Previous analyses of a large number of vehicles typically do not provide safety and goal satisfaction guarantees to the extent that HJ reachability does; however, HJ reachability typically cannot be used to tractably analyze a large number of vehicles. In the second part of this paper, we propose organizing UAVs into platoons, which provides a structure that allows pairwise safety guarantees from HJ reachability to better translate to safety guarantees for the whole platoon. With respect to platooning, we first propose a hybrid systems model of UAVs in platoons to establish the modes of operation needed for our platooning concept. Then, we show how reachability-based controllers can be synthesized to enable UAVs to successfully perform mode switching, as well as prevent dangerous configurations such as collisions. Finally, we show several simulations to illustrate the behavior of UAVs in various scenarios.

Overall, this paper is not meant to provide an exhaustive solution to the unmanned airspace management problem. Instead, this paper illustrates that the computation intractability of HJ reachability can be overcome using an air highway structure with UAVs flying in platoons. In addition, the results are intuitive, which can facilitate human participation in managing the airspace. Although many challenges not addressed in this paper still need to be overcome, this paper can provide a starting point for future research in large-scale UASs with safety and goal satisfaction guarantees.

## II. Air Highways

We consider air highways to be virtual highways in the airspace on which a number of UAV platoons may be present. UAVs seek to arrive at some desired destination starting from their origin by traveling along a sequence of air highways. Air highways are intended to be the common pathways for many UAV platoons, whose members may have different origins and destinations. By routing platoons of UAVs onto a few common pathways, the airspace becomes more tractable to analyze and intuitive to monitor. The concept of platoons will be proposed in Sec. III; in this section, we focus on air highways.

Let an air highway be denoted by the continuous function  $\mathbb{H}: [0, 1] \rightarrow \mathbb{R}^2$ . Such a highway lies in a horizontal plane of fixed altitude, with start and endpoints given by  $\mathbb{H}(0) \in \mathbb{R}^2$  and  $\mathbb{H}(1) \in \mathbb{R}^2$ , respectively. For simplicity, we assume that the highway segment is a straight line segment and the parameter  $s$  indicates the position in some fixed altitude as follows:  $\mathbb{H}(s) = \mathbb{H}(0) + s[\mathbb{H}(1) - \mathbb{H}(0)]$ . To each highway, we assign a speed of travel  $v_{\mathbb{H}}$  and specify the direction of travel to be the direction from  $\mathbb{H}(0)$  to  $\mathbb{H}(1)$ , denoted using a unit vector

$$\hat{d} = \frac{\mathbb{H}(1) - \mathbb{H}(0)}{\|\mathbb{H}(1) - \mathbb{H}(0)\|_2}$$

As we will show in Sec. III, UAVs use simple controllers to track the highway.

Air highways must not only provide structure to make the analysis of a large number of vehicles tractable, but also allow vehicles to reach their destinations while minimizing any relevant costs to the vehicles and to the surrounding regions. Such costs can, for example, take into account people, assets on the ground, and manned aviation, entities to which UAVs pose the biggest risks [3]. Thus, given an origin–destination pair (e.g., two cities), air highways must connect the two points while potentially satisfying other criteria. In addition, optimal air highway locations should ideally be able to be recomputed in real time when necessary to update airspace constraints on the fly, in case, for example, airport configurations change or certain airspaces have to be closed [3]. With this in mind, we now define the air highway placement problem and propose a simple and fast way to approximate its solution that allows for real-time recomputation. Our solution based on solving the Eikonal equation can be thought of as converting a cost map over a geographic area in continuous space into a discrete graph for which the nodes are waypoints joined by edges, which are the air highways.

Note that the primary purpose of this section is to provide a method for the real-time placement of air highways. The specifics of determining the cost map based on population density, geography, weather forecast information, etc., as well as the criteria for when air highway locations need to be updated, is beyond the scope of this paper.

In addition, if vehicles in the airspace are far away from each other, it may be reasonable for all vehicles to fly in an unstructured manner. As long as multiple-way conflicts do not occur, pairwise collision avoidance maneuvers would be sufficient to ensure safety. Unstructured flight is likely to result in more efficient trajectories for each individual vehicle. However, whether multiple-way conflicts occur cannot be predicted ahead of time and are not guaranteed to be resolvable when they occur. By organizing vehicles into platoons, the likelihood of multiple-way conflicts is vastly reduced. Structured flight is, in general, less efficient for the individual vehicle and this loss of efficiency can be thought of as a cost incurred by the vehicles to ensure higher levels of safety.

In general, there may be many different levels of abstractions in the airspace. For larger regions such as cities, air highways may prove beneficial, and for a small region such as a neighborhood, perhaps unstructured flight is sufficiently safe. Further research is needed to better understand parameters, such as the density of vehicles above which unstructured flight is no longer manageable, and other details like platoon size.

### A. Air Highway Placement Problem

Consider a map  $c: \mathbb{R}^2 \rightarrow \mathbb{R}$  which defines the cost  $c(p)$  incurred when a UAV flies over the position  $p = (p_x, p_y) \in \mathbb{R}^2$ . Given any position  $p$ , a large value of  $c(p)$  indicates that the position  $p$  is costly or undesirable for a UAV to fly over. Locations with high cost could, for example, include densely populated areas and areas around airports. In general, the cost map  $c(\cdot)$  may be used to model cost of interference with commercial airspaces, cost of accidents, cost of noise pollution, risks incurred, etc., and can be flexibly specified by government regulation bodies.

Let  $p^o$  denote an origin point and  $p^d$  denote a destination point. Consider a sequence of highways  $\mathbb{S}_N = \{\mathbb{H}_1, \mathbb{H}_2, \dots, \mathbb{H}_N\}$  that satisfies the following:

$$\begin{aligned} \mathbb{H}_1(0) &= p^o \\ \mathbb{H}_i(1) &= \mathbb{H}_{i+1}(0), \quad i = 0, 1, \dots, N-1 \\ \mathbb{H}_N(1) &= p^d \end{aligned} \tag{1}$$

The interpretation of the preceding conditions is that the start point of the first highway is the origin, the endpoint of a highway is the start point of the next highway, and the endpoint of the last highway is the destination. The highways  $\mathbb{H}_1, \dots, \mathbb{H}_N$  form a

sequence of waypoints for a UAV starting at the origin  $p^o$  to reach its destination  $p^d$ .

Given only the origin point  $p^o$  and destination point  $p^d$ , there are an infinite number of choices for a sequence of highways that satisfy Eq. (1). However, if one takes into account the cost of flying over any position  $p$  using the cost map  $c(\cdot)$ , we arrive at the air highway placement problem:

$$\min_{\mathbb{S}_N, N} \left\{ \left( \sum_{i=1}^N \int_0^1 c(\mathbb{H}_i(s)) ds \right) + R(N) \right\} \quad (2)$$

subject to Eq. (1)

where  $R(\cdot)$  is a regularizer, such as  $R(N) = N^2$ .

The interpretation of Eq. (2) is that we consider air highways to be line segments of constant altitude over a region, and UAV platoons travel on these air highways to get from some origin to some destination. Any UAV flying on a highway over some position  $p$  incurs a cost of  $c(p)$ , so that the total cost of flying from the origin to the destination is given by the summation in Eq. (2). The air highway placement problem minimizes the cumulative cost of flying from some origin  $p^o$  to some destination  $p^d$  along the sequence of highways  $\mathbb{S}_N = \{\mathbb{H}_1, \mathbb{H}_2, \dots, \mathbb{H}_N\}$ . The regularization term  $R(N)$  is used to prevent  $N$  from being arbitrarily large.

### B. Eikonal Equation: Cost-Minimizing Path

Let  $s_0, s_1 \in \mathbb{R}$ , and let  $\mathbb{P}: [s_0, s_1] \rightarrow \mathbb{R}^2$  be a path starting from an origin point  $p^o = \mathbb{P}(s_0)$  and ending at a destination point  $p^d = \mathbb{P}(s_1)$ . Note that the sequence  $\mathbb{S}_N$  in Eq. (2) is a piecewise affine example of a path  $\mathbb{P}(s)$ ,  $s \in [s_0, s_1]$ ; however, a path  $\mathbb{P}$  that is not piecewise affine cannot be written as a sequence of highways  $\mathbb{S}_N$ .

More concretely, suppose a UAV flies from an origin point  $p^o$  to a destination point  $p^d$  along some path  $\mathbb{P}(s)$  parametrized by  $s$ . Then,  $\mathbb{P}(s_0) = p^o$  would denote the origin and  $\mathbb{P}(s_1) = p^d$  would denote the destination. All intermediate  $s$  values denote the intermediate positions of the path, that is,  $\mathbb{P}(s) = p(s) = (p_x(s), p_y(s))$ .

Consider the cost map  $c(p_x, p_y)$ , which captures the cost incurred for UAVs flying over the position  $p = (p_x, p_y)$ . Along the entire path  $\mathbb{P}(s)$ , the cumulative cost  $C(\mathbb{P})$  is incurred. Define  $C$  as follows:

$$C(\mathbb{P}) = \int_{s_0}^{s_1} c[\mathbb{P}(s)] ds \quad (3)$$

For an origin–destination pair, we would like to find the path such that the preceding cost is minimized. More generally, given an origin point  $p^o$ , we would like to compute the function  $V$  representing the optimal cumulative cost for any destination point  $p^d$ :

$$V(p^d) = \min_{\mathbb{P}(\cdot), \mathbb{P}(s_1)=p^d} C(\mathbb{P}) = \min_{\mathbb{P}(\cdot), \mathbb{P}(s_1)=p^d} \int_{s_0}^{s_1} c[\mathbb{P}(s)] ds \quad (4)$$

It is well known that the viscosity solution [24] to the Eikonal equation (5) precisely computes the function  $V(p^d)$  given the cost map  $c$  [17,25]. Note that a single function characterizes the minimum cost from an origin  $p^o$  to any destination  $p^d$ . Once  $V$  is found, the optimal path  $\mathbb{P}$  between  $p^o$  and  $p^d$  can be obtained via gradient descent:

$$\begin{aligned} c(p)|\nabla V(p)| &= 1 \\ V(p^o) &= 0 \end{aligned} \quad (5)$$

The Eikonal equation (5) can be efficiently computed numerically using the fast marching method [17]; each computation takes on the order of merely a second.

Note that Eq. (4) can be viewed as a relaxation of the air highway placement problem defined in Eq. (2). Unlike Eq. (2), the relaxation (4) can be quickly solved using currently available numerical tools. Thus, we first solve the approximate air highway placement

problem (4) by solving Eq. (5), and then postprocess the solution to Eq. (4) to obtain an approximation to Eq. (2).

Given a single origin point  $p^o$ , the optimal cumulative cost function  $V(p^d)$  can be computed. Suppose  $M$  different destination points  $p_i^d$ ,  $i = 1, \dots, M$  are chosen. Then,  $M$  different optimal paths  $\mathbb{P}_i$ ,  $i = 1, \dots, M$  are obtained from  $V$ .

### C. From Paths to Waypoints

Each of the cost-minimizing paths  $\mathbb{P}_i$  computed from the solution to the Eikonal equation consists of a closely spaced set of points. Each path  $\mathbb{P}_i$  is an approximation to the sequence of highways

$$\mathbb{S}_{N_i}^i = \left\{ \mathbb{H}_j^i \right\}_{j=1, j=N_i}^{i=M, j=N_i}$$

defined in Eq. (2), but now indexed by the corresponding path index  $i$ .

For each path  $\mathbb{P}_i$ , we would like to sparsify the points on the path to obtain a collection of waypoints  $\mathcal{W}_{i,j}$ ,  $j = 1, \dots, N_i + 1$ , which are the endpoints of the highways:

$$\begin{aligned} \mathbb{H}_j^i(0) &= \mathcal{W}_{i,j}, \\ \mathbb{H}_j^i(1) &= \mathcal{W}_{i,j+1}, \\ j &= 1, \dots, N_i \end{aligned} \quad (6)$$

There are many different ways to do this, and this process will not be our focus. However, for illustrative purposes, we show how this process may be started. We begin by noting the path's heading at the destination point. We add to the collection of waypoints the first point on the path at which the heading changes by some threshold  $\theta_c$ , and repeat this process along the entire path.

If there is a large change in heading within a small section of the cost-minimizing path, then the collection of points may contain many points that are close together. In addition, there may be multiple paths that are very close to each other (in fact, this behavior is desirable), which may contribute to cluttering the airspace with too many waypoints. To reduce clutter, one could cluster the points. Afterward, each cluster of points can be replaced by a single point located at the centroid of the cluster.

To the collection of points resulting from the preceding process, we add the origin and destination points. Repeating the entire process for every path, we obtain waypoints for all the cost-minimizing paths under consideration. Figure 1 summarizes the entire air highway placement process, including our example of how the closely spaced set of points on a path can be sparsified.

### D. Results

To illustrate our air highway placement proposal, we used the San Francisco Bay Area as an example and classified each point on the map into four different regions: regions around airports, highly populated cities, water, and “other.” Each region has an associated cost, reflecting the desirability of flying a vehicle over an area in the region. In general, these costs can be arbitrary and determined by government regulation agencies. For illustration purposes, we assumed the following categories and costs: 1) region around airports,  $c_{\text{airports}} = b$ ; 2) cities,  $c_{\text{cities}} = 1$ ; 3) water,  $c_{\text{water}} = b^{-2}$ ; and 4) other,  $c_{\text{other}} = b^{-1}$ .

This assumption assigns costs in descending order to the categories of regions around airports, cities, other, and water. Flying a UAV in each category is more costly by a factor of  $b$  compared with the next most important category. The factor  $b > 1$  is a tuning parameter that we adjusted to vary the relative importance of the different categories, and we used  $b = 4$  in the following figures.

Figure 2 shows the San Francisco Bay Area geographic map, cost map, cost-minimizing paths, and contours of the value function  $V$ . The region enclosed by the boundary encircling the two plus signs represents the region around airports, which have the highest cost. The dark blue, light blue, and yellow regions (in descending darkness of shading) represent the cities, other, and water categories,

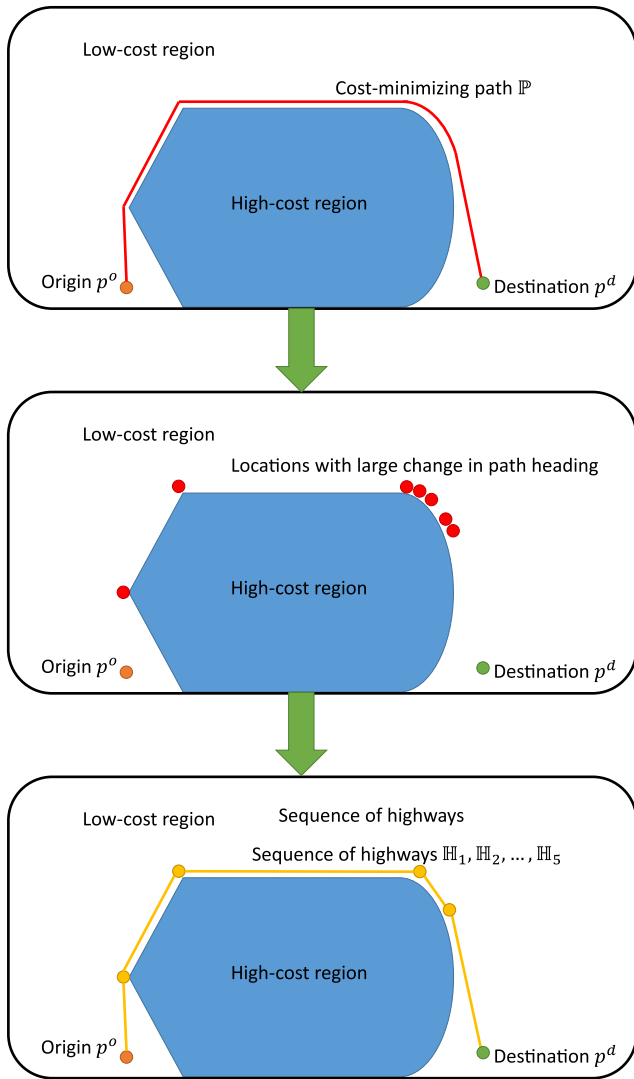


**Fig. 1** Illustration of the air highway placement procedure (color in online).

respectively. We assumed that the origin corresponds to the city “Concord” and chose a number of other major cities as destinations.

A couple of important observations can be made here. First, the cost-minimizing paths to the various destinations in general overlap and only split up when they are very close to entering their destination cities. This is intuitively desirable because having overlapping cost-minimizing paths keeps the number of distinct air highways low. Second, the contours, which correspond to level curves of the value function, have spacings corresponding to the cost map: The spacings are large in areas of low cost and vice versa. This provides insight into the placement of air highways to destinations that were not shown in this example.

Figure 3 shows the result of converting the cost-minimizing paths to a small number of waypoints. The left plot shows the waypoints, interpreted as the start and endpoints of air highways, over a white background for clarity. The right plot shows these air highways over the map of the Bay Area. Note that we could have gone further to merge some of the overlapping highways. However, the purpose of this section is to illustrate the natural occurrence of air highways from cost-minimizing paths; postprocessing of the cost-minimizing paths, which serve as a guide for defining air highways, is not our focus.

### E. Real-Time Highway Location Updates

Because Eq. (5) can be solved in approximately 1 s, the air highway placement process can be redone in real time if the cost map changes at a particular time. This flexibility can be useful in any situation in which unforeseen circumstances could cause a change in the cost of a particular region of the airspace. For example, accidents or disaster response vehicles may result in an area temporarily having a high cost. On the other hand, depending on, for instance, the time of day, it may be most desirable to fly in different regions of the airspace, resulting in those regions temporarily having a low cost.

## III. Unmanned Aerial Vehicle Platooning

Air highways exhibiting trunk routes that separate near destinations motivate the use of platoons that fly on these highways. The air highway structure along with the UAV platooning concept together enable the use of reachability to analyze safety and goal satisfaction properties. The structure reduces the likelihood of multiple-way conflicts and makes pairwise analysis more indicative of the joint safety of all UAVs. In addition to reducing complexity, the

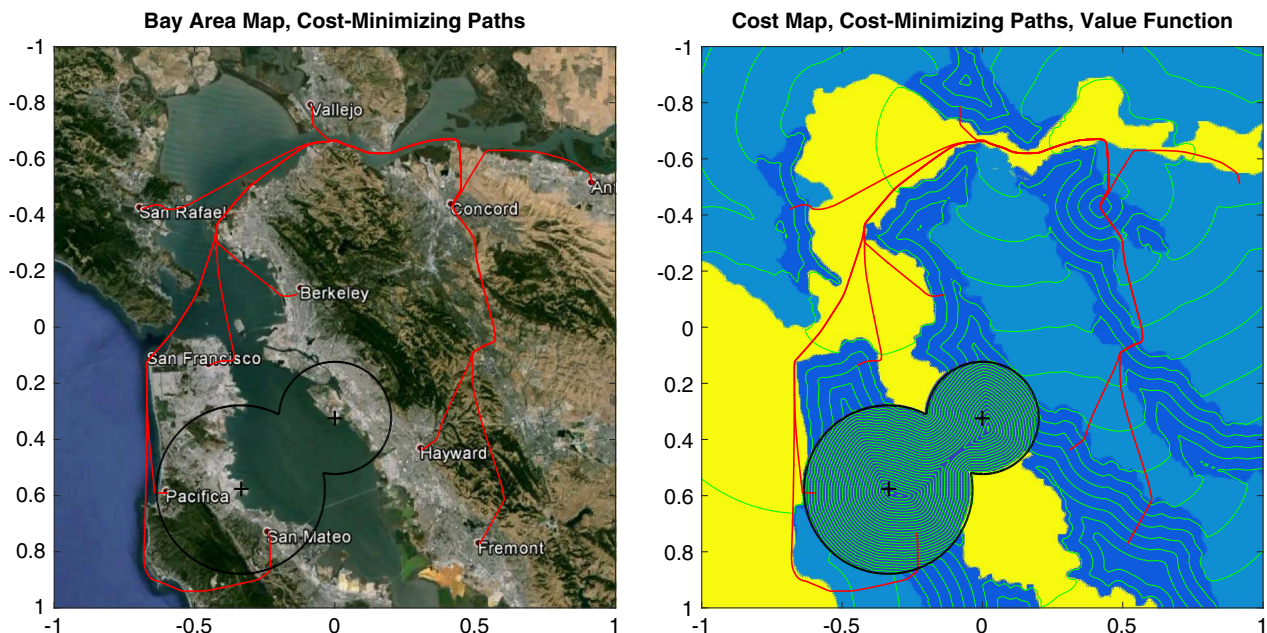


**Fig. 2** Cost-minimizing paths computed by the fast marching method based on the assumed cost map of the San Francisco Bay Area (color in online).



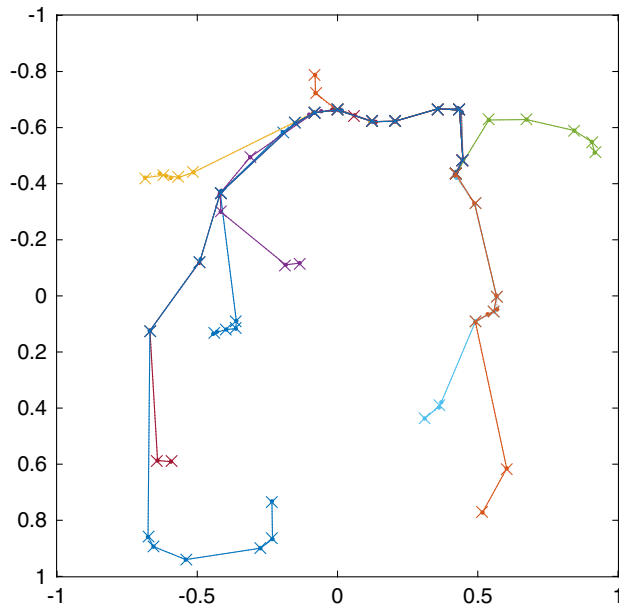


Fig. 3 Results of conversion from cost-minimizing paths to highway way points (color in online).

proposed structure is intuitive and allows human participation in the monitoring and management of the unmanned airspace.

Organizing UAVs into platoons implies that the UAVs cannot fly in an unstructured way and must have a restricted set of controllers or maneuvers depending on the UAV's role in the airspace. To model UAVs flying in platoons on air highways, we propose a hybrid system for which the modes of operations describe a UAV's role in the highway structure. For the hybrid system model, reachability analysis is used to enable successful and safe operation and mode transitions.

#### A. UAVs in Platoons

##### 1. Vehicle Dynamics

Consider a UAV for which the dynamics are given by

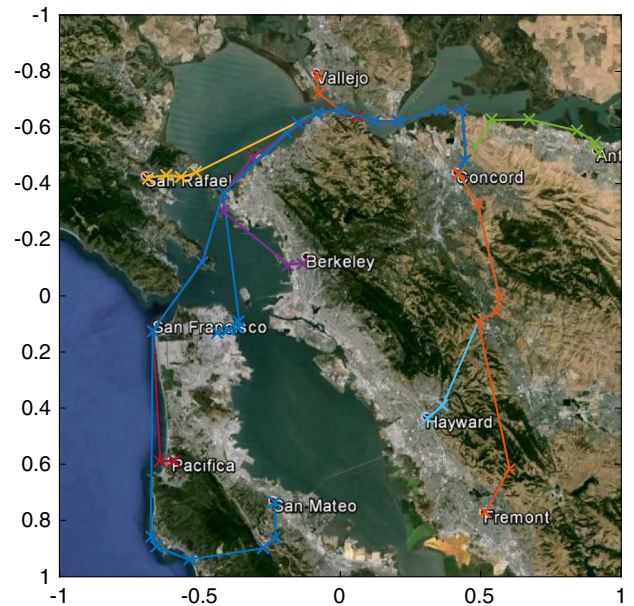
$$\dot{x} = f(x, u) \quad (7)$$

where  $x$  represents the state and  $u$  represents the control action. The techniques we present in this paper do not depend on the dynamics of the vehicles, as long as their dynamics are known. However, for concreteness, we assume that the UAVs are quadrotors that fly at a constant altitude under nonfaulty circumstances. For the quadrotor, we use a simple model in which the  $x$  and  $y$  dynamics are double integrators:

$$\begin{aligned} \dot{p}_x &= v_x \\ \dot{p}_y &= v_y \\ \dot{v}_x &= u_x \\ \dot{v}_y &= u_y \\ |u_x|, |u_y| &\leq u_{\max} \end{aligned} \quad (8)$$

where the state  $x = (p_x, v_x, p_y, v_y) \in \mathbb{R}^4$  represents the quadrotor's position in the  $x$  direction, its velocity in the  $x$ -direction, and its position and velocity in the  $y$  direction, respectively. The control input  $u = (u_x, u_y) \in \mathbb{R}^2$  consists of the acceleration in the  $x$  and  $y$  directions. For convenience, we will denote the position and velocity  $p = (p_x, p_y)$ , and  $v = (v_x, v_y)$ , respectively.

In general, the problem of collision avoidance among  $N$  vehicles cannot be tractably solved using traditional dynamic programming approaches because the computation complexity of these approaches scales exponentially with the number of vehicles. Thus, in our present work, we will consider the situation where UAVs travel on air highways in platoons, defined in the following sections. The structure



imposed by air highways and platooning enables us to analyze the safety and goal satisfaction properties of the vehicles in a tractable manner.

#### 2. Vehicles as Hybrid Systems

We model each vehicle as a hybrid system [21,26] consisting of the modes “free,” “leader,” “follower,” and “faulty.” Within each mode, a vehicle has a set of restricted maneuvers, including one that allows the vehicle to change modes if desired. The modes and maneuvers are as follows.

A free vehicle is not in a platoon or on a highway, and its possible maneuvers or mode transitions are 1) remain a free vehicle by staying away from highways, 2) become a leader by entering a highway to create a new platoon, or 3) become a follower by joining a platoon that is currently on a highway.

A leader vehicle is the vehicle at the front of a platoon (which could consist of only the vehicle itself). The available maneuvers and mode transitions are 1) remain a leader by traveling along the highway at a prespecified speed  $v_{\text{H}}$ , 2) become a follower by merging the current platoon with a platoon in front, or 3) become a free vehicle by leaving the highway.

A follower vehicle is a vehicle that is following a platoon leader. The available maneuvers and mode transitions are 1) remain a follower by staying a distance of  $d_{\text{sep}}$  behind the vehicle in front in the current platoon, 2) remain a follower by joining a different platoon on another highway, 3) become a leader by splitting from the current platoon while remaining on the highway, or 4) become a free vehicle by leaving the highway.

If a vehicle from any of the other modes becomes unable to operate within the allowed set of maneuvers, it transitions into the faulty mode. Reasons for transitioning to the faulty mode include vehicle malfunctions, performing collision avoidance with respect to another faulty vehicle, etc. A faulty vehicle is assumed to descend via a fail-safe mechanism after some prespecified duration  $t_{\text{faulty}}$  to a different altitude level where it no longer poses a threat to vehicles on the air highway system.

Such a fail-safe mechanism could be an emergency landing procedure such as those analyzed in [27–29]. Typically, emergency landing involves identifying the type of fault and finding feasible landing locations given the dynamics during the fault. We will omit these details and summarize them into  $t_{\text{faulty}}$ , the time required to exit the current altitude level.

The available maneuvers and associated mode transitions are summarized in Fig. 4. Suppose that there are  $N$  vehicles in total in the airspace containing the highway system. We will denote the  $N$

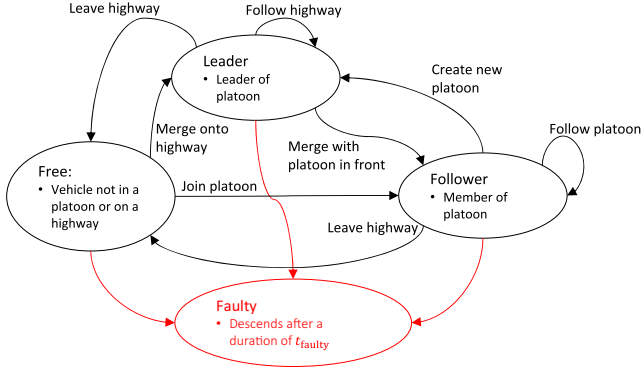


**Fig. 4** Hybrid modes for vehicles in platoons. Vehicles begin in the free mode before they enter the highway (color in online).

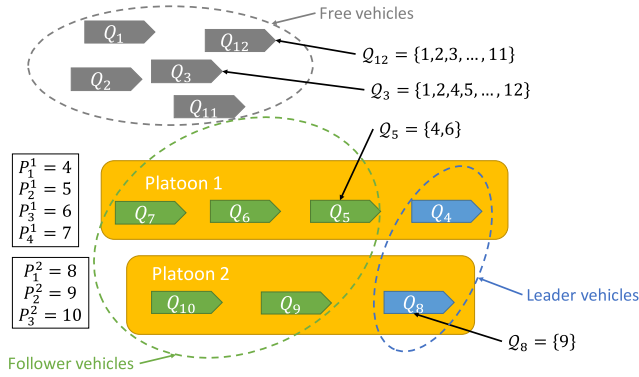


**Fig. 5** Notation for vehicles in platoons (color in online).

vehicles as  $Q_i$ ,  $i = 1 \dots N$ . We consider a platoon of vehicles to be a group of  $M$  vehicles ( $M \leq N$ ), denoted  $Q_{P_1}, \dots, Q_{P_M}$ ,  $\{P_j\}_{j=1}^M \subseteq \{i\}_{i=1}^N$ , in a single-file formation. When necessary, we will use superscripts to denote vehicles of different platoons:  $Q_{P_i^j}$  represents the  $i$ th vehicle in the  $j$ th platoon.

For convenience, let  $Q_i$  denote the set of indices of vehicles with respect to which  $Q_i$  checks safety. If vehicle  $Q_i$  is a free vehicle, then it must check for safety with respect to all other vehicles,  $Q_i = \{j: j \neq i\}$ . If the vehicle is part of a platoon, then it checks safety with respect to the platoon member in front and behind,  $Q_i = \{P_{j+1}, P_{j-1}\}$ . Figure 5 summarizes the indexing system of the vehicles.

We will organize the vehicles into platoons traveling along air highways. The vehicles maintain a separation distance of  $d_{\text{sep}}$  with their neighbors inside the platoon. To allow for close proximity of the vehicles and the ability to resolve multiple simultaneous safety breaches, we assume that, when a vehicle exhibits unpredictable behavior, it will be able to exit the altitude range of the highway within a duration of  $t_{\text{faulty}}$ . Such a requirement may be implemented practically as a fail-safe mechanism to which the vehicles revert when needed.

### 3. Objectives

Given the preceding modeling assumptions, our goal is to provide control strategies to guarantee the success and safety of all the mode transitions. The theoretical tool used to provide the safety and goal satisfaction guarantees is reachability. The BRSs we compute will allow each vehicle to perform complex actions, such as to merge onto a highway to form a platoon, join a new platoon, leave a platoon to create a new one, or react to malfunctioning or intruder vehicles.

We also propose more basic controllers to perform other simpler actions, such as to follow the highway at constant altitude at a specified speed or maintain a constant relative position and velocity with respect to the leader of a platoon.

In general, the control strategy of each vehicle has a safety component, which specifies a set of states that it must avoid, and a

goal satisfaction component, which specifies a set of states that the vehicle aims to reach. Together, the safety and goal satisfaction controllers guarantee the safety and success of a vehicle in the airspace making any desired mode transition. In this paper, these guarantees are provided using reachability analysis, and allow the multi-UAV system to perform joint maneuvers essential to maintaining structure in the airspace.

## B. Hamilton–Jacobi Reachability

### 1. General Framework

Consider a differential game between two players described by the system

$$\dot{x} = f(x, u_1, u_2), \quad \text{for almost every } t \in [-T, 0] \quad (9)$$

where  $x \in \mathbb{R}^n$  is the system state,  $u_1 \in \mathcal{U}_1$  is the control of player 1, and  $u_2 \in \mathcal{U}_2$  is the control of player 2. We assume  $f: \mathbb{R}^n \times \mathcal{U}_1 \times \mathcal{U}_2 \rightarrow \mathbb{R}^n$  is uniformly continuous, bounded, and Lipschitz continuous in  $x$  for fixed  $u_1, u_2$ , and the control functions  $u_1(\cdot) \in \mathcal{U}_1, u_2(\cdot) \in \mathcal{U}_2$  are drawn from the set of measurable functions.<sup>†</sup> Player 2 is allowed to use nonanticipative strategies  $\gamma$  [30,31], defined by

$$\begin{aligned} \gamma \in \Gamma &:= \{\mathcal{N}: \mathcal{U}_1 \rightarrow \mathcal{U}_2 | u_1(r) = \hat{u}_1(r) \\ &\text{for almost every } r \in [t, s] \rightarrow \mathcal{N}[u_1](r) \\ &= \mathcal{N}[\hat{u}_1](r) \text{ for almost every } r \in [t, s]\} \end{aligned} \quad (10)$$

In our differential game, the goal of player 2 is to drive the system into some target set  $\mathcal{L}$ , and the goal of player 1 is to drive the system away from it. The set  $\mathcal{L}$  is represented as the zero sublevel set of a bounded, Lipschitz continuous function  $l: \mathbb{R}^n \rightarrow \mathbb{R}$ . We call  $l(\cdot)$  the *implicit surface function* representing the set  $\mathcal{L}: \mathcal{L} = \{x \in \mathbb{R}^n | l(x) \leq 0\}$ .

Given the dynamics (8) and the target set  $\mathcal{L}$ , we would like to compute the BRS  $\mathcal{V}(t)$ :

$$\begin{aligned} \mathcal{V}(t) &:= \{x \in \mathbb{R}^n | \exists \gamma \in \Gamma \text{ such that } \forall u_1(\cdot) \in \mathcal{U}_1, \\ &\exists s \in [t, 0], \xi_f(s; t, x, u_1(\cdot), \gamma[u_1](\cdot)) \in \mathcal{L}\} \end{aligned} \quad (11)$$

where  $\xi_f$  is the trajectory of the system satisfying initial conditions  $\xi_f(t; x, t, u_1(\cdot), u_2(\cdot)) = x$  and the following differential equation almost everywhere on  $[-t, 0]$ :

$$\frac{d}{ds} \xi_f(s; x, t, u_1(\cdot), u_2(\cdot)) = f(\xi_f(s; x, t, u_1(\cdot), u_2(\cdot)), u_1(s), u_2(s)) \quad (12)$$

Many methods involving solving HJ PDEs [9] and HJ variational inequalities (VIs) [8,10,11] have been developed for computing the BRS. These HJ PDEs and HJ VIs can be solved using well-established numerical methods. For this paper, we use the formulation in [9], which shows that the BRS  $\mathcal{V}(t)$  can be obtained as the zero sublevel set of the viscosity solution [24]  $V(t, x)$  of the following terminal value HJ PDE:

$$\begin{aligned} D_t V(t, x) + \min \left\{ 0, \max_{u_1 \in \mathcal{U}_1} \min_{u_2 \in \mathcal{U}_2} D_x V(t, x) \cdot f(x, u_1, u_2) \right\} &= 0, \\ V(0, x) &= l(x) \end{aligned} \quad (13)$$

from which we obtain  $\mathcal{V}(t) = \{x \in \mathbb{R}^n | V(t, x) \leq 0\}$ . The target set, reachable set, and implicit surface functions  $l(x)$  and  $V(t, x)$  representing them are shown in Fig. 6. From the solution  $V(t, x)$ , we can also obtain the optimal controls for both players via the following:

<sup>†</sup>A function  $f: X \times Y \rightarrow Z$  between two measurable spaces  $(X, \Sigma_X)$  and  $(Y, \Sigma_Y)$  is said to be measurable if the preimage of a measurable set in  $Z$  is a measurable set in  $X$ , that is,  $\forall V \in \Sigma_Z, f^{-1}(V) \in \Sigma_X$ , with  $\Sigma_X, \Sigma_Y, \Sigma_Z$   $\sigma$ -algebras on  $X, Y, Z$ .

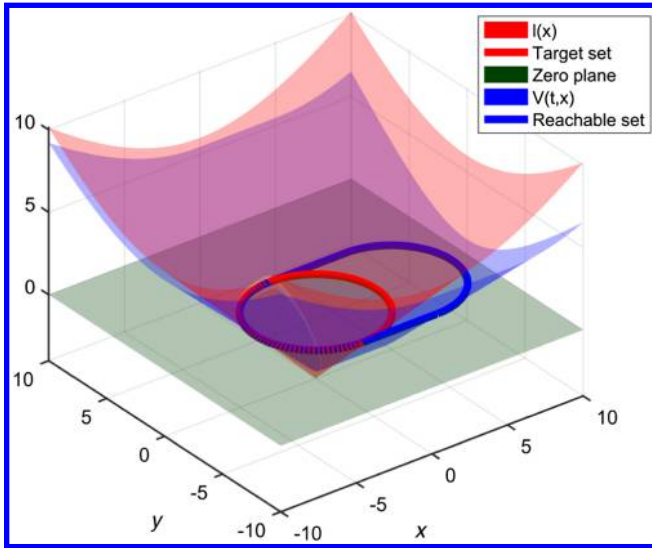


Fig. 6 Illustration of a target set, a BRS, and their implicit surface functions (color in online).

$$\begin{aligned} u_1^*(t, x) &= \arg \max_{u_1 \in \mathcal{U}_1} \min_{u_2 \in \mathcal{U}_2} D_x V(t, x) \cdot f(x, u_1, u_2) \\ u_2^*(t, x) &= \arg \min_{u_2 \in \mathcal{U}_2} D_x V(t, x) \cdot f(x, u_1^*, u_2) \end{aligned} \quad (14)$$

In the special case where there is only one player, we obtain an optimal control problem for a system with dynamics

$$\dot{x} = f(x, u), \quad t \in [-T, 0], \quad u \in \mathcal{U} \quad (15)$$

The BRS in this case would be given by the HJ PDE

$$\begin{aligned} D_t V(t, x) + \min_{u \in \mathcal{U}} \left\{ 0, \min_{u \in \mathcal{U}} D_x V(t, x) \cdot f(x, u) \right\} &= 0 \\ V(0, x) &= l(x) \end{aligned} \quad (16)$$

where the optimal control is given by

$$u^*(t, x) = \arg \min_{u \in \mathcal{U}} D_x V(t, x) \cdot f(x, u) \quad (17)$$

For our application, we will use several decoupled system models and use decomposition techniques [32–34], which enables real-time four-dimensional (4-D) BRS computations and tractable six-dimensional (6-D) BRS computations.

## 2. Relative Dynamics and Augmented Relative Dynamics

Besides Eq. (8), we will also consider the relative dynamics between two quadrotors  $Q_i, Q_j$ . These dynamics can be obtained by defining the relative variables

$$\begin{aligned} p_{x,r} &= p_{x,i} - p_{x,j} \\ p_{y,r} &= p_{y,i} - p_{y,j} \\ v_{x,r} &= v_{x,i} - v_{x,j} \\ v_{y,r} &= v_{y,i} - v_{y,j} \end{aligned} \quad (18)$$

We treat  $Q_i$  as player 1, the evader who wishes to avoid collision, and we treat  $Q_j$  as player 2, the pursuer, or disturbance, who wishes to cause a collision. In terms of the relative variables given in Eq. (18), we have

$$\begin{aligned} \dot{p}_{x,r} &= v_{x,r} \\ \dot{p}_{y,r} &= v_{y,r} \\ \dot{v}_{x,r} &= u_{x,i} - u_{x,j} \\ \dot{v}_{y,r} &= u_{y,i} - u_{y,j} \end{aligned} \quad (19)$$

We also augment Eq. (18) with the velocity of  $Q_i$ , given in Eq. (20), to impose a velocity limit on the quadrotor.

$$\begin{aligned} \dot{p}_{x,r} &= v_{x,r} \\ \dot{p}_{y,r} &= v_{y,r} \\ \dot{v}_{x,r} &= u_{x,i} - u_{x,j} \\ \dot{v}_{y,r} &= u_{y,i} - u_{y,j} \\ \dot{v}_{x,i} &= u_{x,i} \\ \dot{v}_{y,i} &= u_{y,i} \end{aligned} \quad (20)$$

## C. Reachability-Based Controllers

Reachability analysis is useful for constructing controllers in a large variety of situations. To construct different controllers, an appropriate target set needs to be defined depending on the goal of the controller. If one defines the target set to be a set of desired states, the BRS would represent the states that a system needs to first arrive at to reach the desired states. On the other hand, if the target set represents a set of undesirable states, then the BRS would indicate the region of the state space that the system needs to avoid. In addition, the system dynamics with which the BRS is computed provide additional flexibility when using reachability to construct controllers.

Using a number of different target sets and dynamics, we now propose different reachability-based controllers used for vehicle mode transitions in our platooning concept.

### 1. Getting to a Target State

The controller used by a vehicle to reach a target state is important in two situations in the platooning context. First, a vehicle in the free mode can use the controller to merge onto a highway, forming a platoon and changing modes to a leader vehicle. Second, a vehicle in either the leader mode or the follower mode can use this controller to change to a different highway, becoming a leader vehicle.

In both of the preceding cases, we use the dynamics of a single vehicle specified in Eq. (8). The target state would be a position  $(\bar{p}_x, \bar{p}_y)$  representing the desired merging point on the highway, along with a velocity  $(\bar{v}_x, \bar{v}_y) = v_H$ , which corresponds to the speed and direction of travel specified by the highway. For the reachability computation, we define the target set to be a small range of states around the target state  $\bar{x}_H = (\bar{p}_x, \bar{p}_y, \bar{v}_x, \bar{v}_y)$ :

$$\begin{aligned} \mathcal{L}_H &= \left\{ x: |p_x - \bar{p}_x| \leq r_{p_x}, |v_x - \bar{v}_x| \leq r_{v_x}, \right. \\ &\quad \left. |p_y - \bar{p}_y| \leq r_{p_y}, |v_y - \bar{v}_y| \leq r_{v_y} \right\} \end{aligned} \quad (21)$$

Here, we represent the target set  $\mathcal{L}_H$  as the zero sublevel set of the function  $l_H(x)$ , which specifies the terminal condition of the HJ PDE that we need to solve. Once the HJ PDE is solved, we obtain the BRS  $\mathcal{V}_H(t)$  from the subzero level set of the solution  $V_H(t, x)$ . More concretely,  $\mathcal{V}_H(T) = \{x: V_H(-T, x) \leq 0\}$  is the set of states from which the system can be driven to the target  $\mathcal{L}_H$  within a duration of  $T$ .

Depending on the time horizon  $T$ , the size of the BRS  $\mathcal{V}_H(T)$  varies. In general, a vehicle may not initially be inside the BRS  $\mathcal{V}_H(T)$ , yet it needs to be to get to its desired target state. Determining a control strategy to reach  $\mathcal{V}_H(T)$  is itself a reachability problem [with  $\mathcal{V}_H(T)$  as the target set], and it would seem like this reachability problem needs to be solved for us to use the results from our first reachability problem. However, practically, one could choose  $T$  to be large enough to cover a sufficiently large area to include any

practically conceivable initial state. From our simulations, a suitable algorithm for getting to a desired target state is as follows:

1) Move toward  $\bar{x}_H$  in pure pursuit with some velocity, until  $V_H(-T, x) \leq 0$ . In practice, this step consistently drives the system into the BRS.

2) Apply the optimal control extracted from  $V_H(-T, x)$  according to Eq. (17) until  $\mathcal{L}_H$  is reached.

### 2. Getting to a State Relative to Another Vehicle

In the platooning context, being able to go to a state relative to another moving vehicle is important for the purpose of forming and joining platoons. For example, a free vehicle may join an existing platoon that is on a highway and change modes to become a follower. Also, a leader or follower may join another platoon and afterward go into the follower mode.

To construct a controller for getting to a state relative to another vehicle, we use the relative dynamics of two vehicles, given in Eq. (19). In general, the target state is specified to be some position  $(\bar{p}_{x,r}, \bar{p}_{y,r})$  and velocity  $(\bar{v}_{x,r}, \bar{v}_{y,r})$  relative to a reference vehicle. In the case of a vehicle joining a platoon that maintains a single file, the reference vehicle would be the platoon leader, the desired relative position would be a certain distance behind the leader, depending on how many other vehicles are already in the platoon; the desired relative velocity would be  $(0, 0)$  so that the formation can be kept.

For the reachability problem, we define the target set to be a small range of states around the target state  $\bar{x}_P = (\bar{p}_{x,r}, \bar{p}_{y,r}, \bar{v}_{x,r}, \bar{v}_{y,r})$ :

$$\mathcal{L}_P = \left\{ x: |p_{x,r} - \bar{p}_{x,r}| \leq r_{p_x}, |v_{x,r} - \bar{v}_{x,r}| \leq r_{v_x}, \right. \\ \left. |p_{y,r} - \bar{p}_{y,r}| \leq r_{p_y}, |v_{y,r} - \bar{v}_{y,r}| \leq r_{v_y} \right\} \quad (22)$$

The target set  $\mathcal{L}_P$  is represented by the zero sublevel set of the implicit surface function  $l_P(x)$ , which specifies the terminal condition of the HJ PDE (13). The zero sublevel set of the solution to Eq. (13),  $V_P(-T, x)$ , gives us the set of relative states from which a quadrotor can reach the target in the relative coordinates within a duration of  $T$ . In the BRS computation, we assume that the reference vehicle moves along the highway at constant speed, so that  $u_j(t) = 0$ . The following is a suitable algorithm for a vehicle joining a platoon to follow the platoon leader:

1) Move toward  $\bar{x}_P$  in a straight line, with some velocity, until  $V_P(-T, x) \leq 0$ .

2) Apply the optimal control extracted from  $V_P(-T, x)$  according to Eq. (14) until  $\mathcal{L}_P$  is reached.

### 3. Avoiding Collisions

A vehicle can use a goal satisfaction controller described in the previous sections when it is not in any danger of collision with other vehicles. If the vehicle could potentially be involved in a collision within the next short period of time, it must switch to a safety controller. The safety controller is available in every mode, and executing the safety controller to perform an avoidance maneuver does not change a vehicle's mode.

In the context of our platooning concept, we define an unsafe configuration as follows: a vehicle is either within a minimum separation distance  $d$  to a reference vehicle in both the  $x$  and  $y$  directions, or is traveling with a speed above the speed limit  $v_{\max}$  in either of the  $x$  and  $y$  directions. To take this specification into account, we use the augmented relative dynamics given by Eq. (20) for the reachability problem and define the target set as follows:

$$\mathcal{L}_S = \left\{ x: |p_{x,r}|, |p_{y,r}| \leq d \vee |v_{x,i}| \geq v_{\max} \vee |v_{y,i}| \geq v_{\max} \right\} \quad (23)$$

We can now define the implicit surface function  $l_S(x)$  corresponding to  $\mathcal{L}_S$ , and solve the HJ PDE (13) using  $l_S(x)$  as the terminal condition. As before, the zero sublevel set of the solution  $V_S(t, x)$  specifies the BRS  $\mathcal{V}_S(t)$ , which characterizes the states in the augmented relative coordinates, as defined in Eq. (20), from which  $Q_i$  cannot avoid  $\mathcal{L}_S$  for a time period of  $t$ , if  $Q_j$  uses the worst-case

control. To avoid collisions,  $Q_i$  must apply the safety controller according to Eq. (14) on the boundary of the BRS to avoid going into the BRS. The following algorithm wraps our safety controller around goal satisfaction controllers:

1) For a specified time horizon  $t$ , evaluate  $V_S(-t, x_i - x_j)$  for all  $j \in Q(i)$ .

$Q(i)$  is the set of quadrotors with which vehicle  $Q_i$  checks safety.

2) Use the safety or goal satisfaction controller depending on the values  $V_S(-t, x_i - x_j)$ ,  $j \in Q(i)$ :

If  $\exists j \in Q(i)$ ,  $V_S(-t, x_i - x_j) \leq 0$ , then  $Q_i, Q_j$  are in potential conflict, and  $Q_i$  must use a safety controller; otherwise,  $Q_i$  may use a goal satisfaction controller.

### D. Other Controllers

Reachability was used in Sec. III.C for the relatively complex maneuvers that require safety and goal satisfaction guarantees. For the simpler maneuvers of traveling along a highway and following a platoon, many well-known classical controllers suffice. For illustration, we use the simple controllers described next.

#### 1. Traveling Along a Highway

We use a model-predictive controller for traveling along a highway; this controller allows the leader to travel along a highway at a prespecified speed. Here, the goal is for a leader vehicle to track an air highway  $\mathbb{H}(s)$ ,  $s \in [0, 1]$ , while maintaining some constant velocity  $v_{\mathbb{H}}$  specified by the highway. The highway and the specified velocity can be written as a desired position and velocity over time  $\bar{p}(t), \bar{v}(t)$ . Assuming that the initial position on the highway  $s_0 = s(t_0)$  is specified, such a controller can be obtained from the following optimization problem over the time horizon  $[t_0, t_1]$ :

minimize

$$\int_{t_0}^{t_1} \{ \|p(t) - \bar{p}(t)\|_2 + \|v(t) - \bar{v}(t)\|_2 + 1 - s \} dt$$

subject to vehicle dynamics (7)

$$|u_x|, |u_y| \leq u_{\max}, |v_x|, |v_y| \leq v_{\max} \\ s(t_0) = s_0, \dot{s} \geq 0 \quad (24)$$

If we discretize time, the preceding optimization becomes convex optimization over a small number of decision variables and can be quickly solved.

#### 2. Following a Platoon

Follower vehicles use a feedback control law tracking a nominal position and velocity in the platoon, with an additional feedforward term given by the leader's acceleration input; here, for simplicity, we assume perfect communication between the leader and follower vehicles. This following law enables smooth vehicle trajectories in the relative platoon frame, while allowing the platoon as a whole to perform agile maneuvers by transmitting the leader's acceleration command  $u_{P_1}(t)$  to all vehicles.

The  $i$ th member of the platoon  $Q_{P_i}$  is expected to track a relative position in the platoon  $r^i = (r_x^i, r_y^i)$  with respect to the leader's position  $p_{P_1}$  and the leader's velocity  $v_{P_1}$  at all times. The resulting control law has the form:

$$u^i(t) = k_p[p_{P_1}(t) + r^i(t) - p^i(t)] + k_v[v_{P_1}(t) - v^i(t)] + u_{P_1}(t) \quad (25)$$

for some  $k_p, k_v > 0$ . In particular, a simple rule for determining  $r^i(t)$  in a single-file platoon is given for  $Q_{P_i}$  as

$$r^i(t) = -(i-1)d_{\text{sep}}\hat{d} \quad (26)$$

where  $d_{\text{sep}}$  is the spacing between vehicles along the platoon and  $\hat{d}$  is the highway's direction of travel.



### E. Summary of Controllers

We have introduced several reachability-based controllers, as well as some simple controllers. Pairwise collision avoidance is guaranteed using the safety controller, described in Sec. III.C.3. As long as a vehicle is not in potential danger according to the safety BRSSs, it is free to use any other controller. All of these other controllers are *goal satisfaction controllers*, and their corresponding mode transitions are shown in Fig. 7.

The controller for getting to an absolute target state, described in Sec. III.C.1, is used whenever a vehicle needs to move onto a highway to become a platoon leader. This controller guarantees the success of the mode transitions shown in blue in Fig. 7.

The controller for getting to a relative target state, described in Sec. III.C.2, is used whenever a vehicle needs to join a platoon to become a follower. This controller guarantees the success of the mode transitions shown in green in Fig. 7.

For the simple maneuvers of traveling along a highway or following a platoon, many simple controllers such as the ones suggested in Sec. III.D can be used. These controllers keep the vehicles in either the leader or the follower mode. Alternatively, additional controllers can be designed for exiting the highway, although these are not considered in this paper. All of these nonreachability-based controllers are shown in gray in Fig. 7.

### F. Safety Analysis

Under normal operations in a single platoon, each follower vehicle  $Q_i$ ,  $i = P_2, \dots, P_{M-1}$  in a platoon checks whether it is in the safety BRS with respect to  $Q_{P_{i-1}}$  and  $Q_{P_{i+1}}$ , and so  $Q_i = \{P_{i+1}, P_{i-1}\}$  for  $i = P_2, \dots, P_{N-1}$ . Assuming there are no nearby vehicles outside of the platoon, the platoon leader  $Q_{P_1}$  checks safety against  $Q_{P_2}$ , and the platoon trailer  $Q_{P_N}$  checks safety against  $Q_{P_{N-1}}$ , and so  $Q_{P_1} = \{P_2\}$ ,  $Q_{P_N} = \{P_{N-1}\}$ . When all vehicles are using goal satisfaction controllers to perform their allowed maneuvers, in most situations, no pair of vehicles should be in an unsafe configuration. However, occasionally a vehicle  $Q_k$  may behave unexpectedly due to faults or malfunctions, in which case it may come into an unsafe configuration with another vehicle.

With our choice of  $Q_i$  and the assumption that the platoon is in a single-file formation, some vehicle  $Q_i$  would get near the safety BRS with respect to  $Q_k$ , where  $Q_k$  is likely to be the vehicle in front of or behind  $Q_i$ . In this case, a “safety breach” occurs. Our synthesis of the safety controller guarantees the following: between every pair of vehicles  $Q_i, Q_k$ , if  $V_S(-t, x_i - x_k) > 0$ , then  $\exists u_i$  to keep  $Q_i$  from colliding with  $Q_k$  for a desired time horizon  $t$ , despite the worst-case (an adversarial) control from  $Q_k$ . Therefore, as long as the number of safety breaches is at most one for  $Q_i$ ,  $Q_i$  can simply use the optimal control to avoid  $Q_k$  and avoid collision for the time horizon of  $t$ . Under the assumption that vehicles are able to exit the current altitude range within a duration of  $t_{\text{faulty}}$ , if we choose  $t = t_{\text{faulty}}$ , the safety breach would always end before any collision can occur.

Within a duration of  $t_{\text{faulty}}$ , there is a small chance that additional safety breaches may occur. However, as long as the total number of safety breaches does not exceed the number of affected vehicles, collision avoidance of all the vehicles can be guaranteed for the duration  $t_{\text{faulty}}$ . However, as our simulation results show, placing vehicles in single-file platoons makes the likelihood of multiple safety breaches low during the presence of one intruder vehicle.

In the event that multiple safety breaches occur for some of the vehicles due to a malfunctioning vehicle within the platoon or intruding vehicles outside of the platoon, vehicles that are causing safety breaches must exit the highway altitude range to avoid collisions. Every extra altitude range reduces the number of simultaneous safety breaches by one, and so  $K$  simultaneous safety breaches can be resolved using  $K - 1$  different altitude ranges. The general process and details of the complete picture of multi-altitude collision avoidance is part of our future work.

The concept of platooning can be coupled with any collision avoidance algorithm that provides safety guarantees. In this paper, we have only proposed the simplest reachability-based collision avoidance scheme. Existing collision avoidance algorithms such as those in [35,36] have the potential to provide safety guarantees for many vehicles to resolve multiple safety breaches at once. Coupling the platooning concept with the more advanced collision avoidance methods that provide guarantees for a larger number of vehicles would reduce the risk of multiple safety breaches.

Given that vehicles within a platoon are safe with respect to each other, each platoon can be treated as a single vehicle and perform collision avoidance with other platoons when needed. The option of treating each platoon as a single unit can reduce the number of individual vehicles that need to check for safety against each other, reducing overall computation burden.

### G. Numerical Simulations

In this section, we consider several situations that vehicles in a platoon on an air highway may commonly encounter and show via simulations the behaviors that emerge from the controllers we defined in Secs. III.C and III.D.

#### 1. Forming a Platoon

We first consider the scenario in which free vehicles merge onto an initially unoccupied highway. To do this, each vehicle first checks safety with respect to all other vehicles and uses the safety controller if necessary, according to Sec. III.C.3. Otherwise, the vehicle uses the goal satisfaction controller for getting to an absolute target set described in Sec. III.C.1 to merge onto the highway, create a platoon, and become a leader vehicle if there are no platoons on the highway. If there is already a platoon on the highway, then the vehicle would use the goal satisfaction controller for getting to a target set relative to the platoon leader as described in Sec. III.C.2 to join the platoon and become a follower.

For the simulation example, shown in Fig. 8, the highway is specified by a line segment beginning at the origin. The five vehicles,  $Q_1, Q_2, \dots, Q_5$  are shown as small disks with an arrow indicating their heading, and colored orange, purple, light blue, dark blue, and yellow, respectively. The first two plots in Fig. 8 illustrate the use of safety and goal satisfaction BRS for the first two vehicles. Because the goal satisfaction BRSs are in 4-D and the safety BRSs are in 6-D, we compute and plot their two-dimensional slices based on the vehicles' velocities and relative velocities. All vehicles begin as free vehicles, and so they each need to take into account five different BRSs: four safety BRSs and one goal satisfaction BRS. For clarity, we only show the goal satisfaction BRS and the four safety BRSs for one of the vehicles.

For  $Q_1$  (orange, vehicle closest to highway at  $t = 4.2$ ), an arbitrary point of entry on the highway is chosen as the target absolute position, and the velocity corresponding to a speed of 10 m/s in the direction of the highway is chosen as the target absolute velocity. This forms the target state  $\bar{x}_H = (\bar{p}_x, \bar{v}_x, \bar{p}_y, \bar{v}_y)$ , from which we define the target set  $\mathcal{L}_H$  as in Sec. III.C.1.

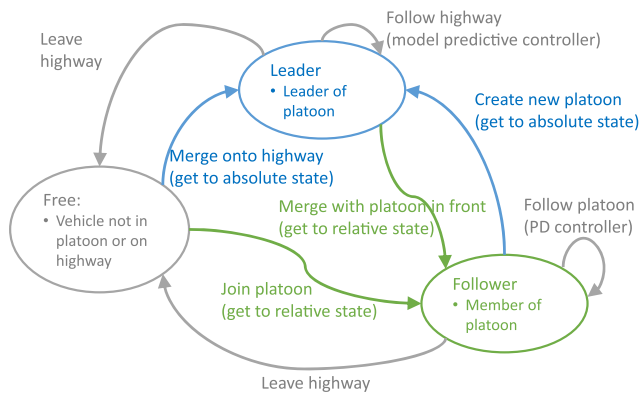


**Fig. 7 Summary of mode switching controllers. Reachability-based controllers are shown as the blue and green arrows pointing towards the Leader and Follower modes, respectively (color in online).**

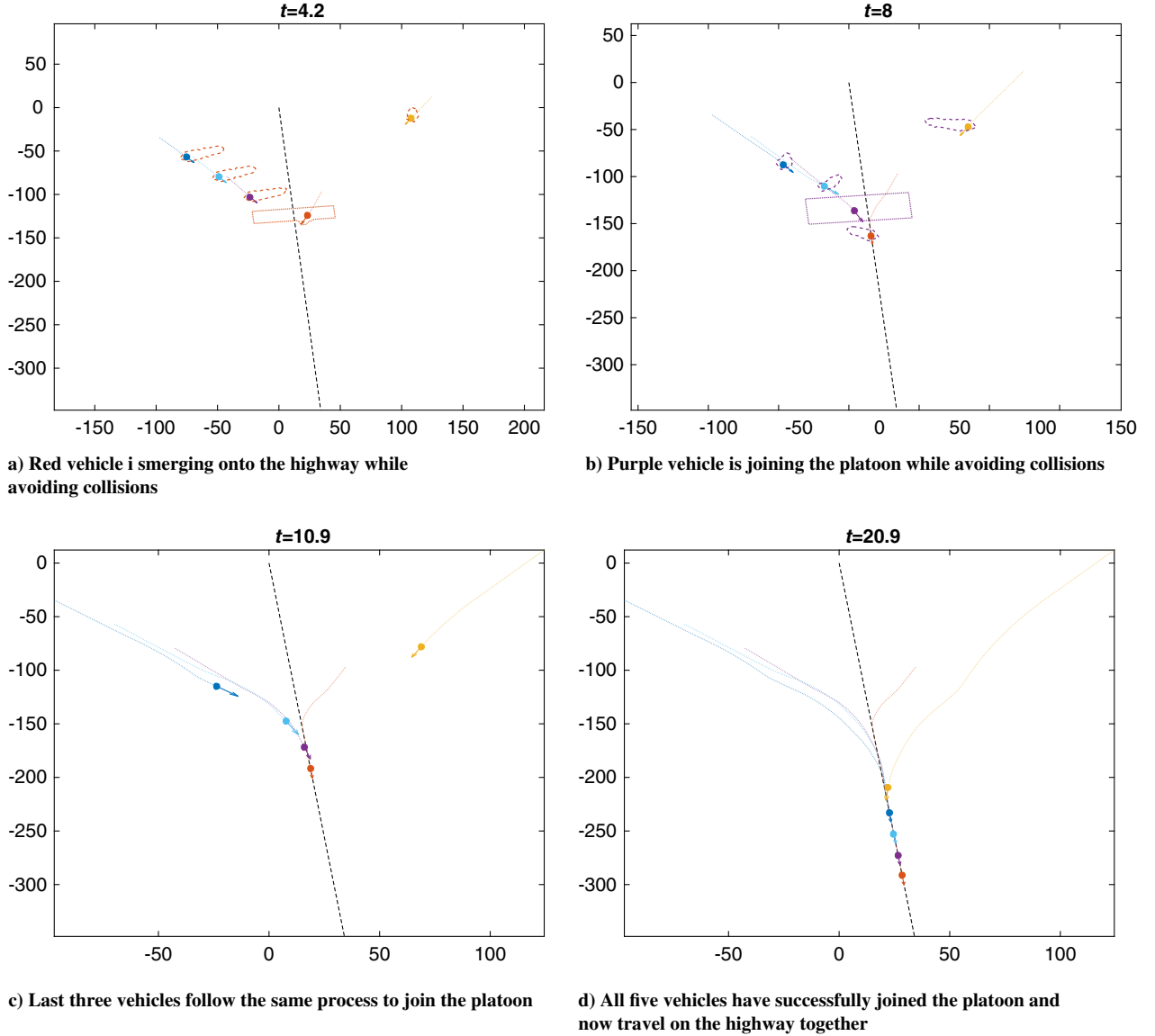


**Fig. 8** Simulation showing how five vehicles initially in the free mode can form a platoon (color in online).

At  $t = 4.2$ ,  $Q_1$  (orange) is inside the goal satisfaction BRS for getting to an absolute state, shown as the dotted orange boundary. Therefore, it is “locked in” to the target state  $\bar{x}_H$  and follows the optimal control in Eq. (17) to  $\bar{x}_H$ . During the entire time,  $Q_1$  checks whether it may collide with any of the other vehicles within a time horizon of  $t_{\text{faulty}}$ . To do this, it simply checks whether its state relative to each of the other vehicles is within the corresponding safety BRS. As an example, the safety BRS boundary with respect to  $Q_2$  (purple, next closest vehicle to the highway at  $t = 4.2$ ) is shown as the orange dashed boundary around  $Q_2$  (purple);  $Q_1$  (orange) is safe with respect to  $Q_2$  (purple) because  $Q_1$  (orange) is outside of the boundary. In fact,  $Q_1$  is safe with respect to all vehicles.

After completing merging onto the empty highway,  $Q_1$  (orange, now on the highway at  $t = 8$ ) creates a platoon and becomes its leader, whereas subsequent vehicles begin to form a platoon behind the leader in the order of ascending distance to  $Q_1$  (orange) according to the process described in Sec. III.C.2. Here, we choose the target relative position  $(\bar{p}_{x,r}, \bar{p}_{y,r})$  to be a distance  $d_{\text{sep}}$  behind the last reserved slot in the platoon and the target relative velocity  $(\bar{v}_{x,r}, \bar{v}_{y,r}) = (0, 0)$  with respect to the leader to maintain the platoon formation. This gives us the target set  $\mathcal{L}_P$  that we need.

At  $t = 8.0$ ,  $Q_2$  (purple, vehicle closest but not on the highway) is in the process of joining the platoon behind  $Q_1$  (orange) by moving toward the target  $\bar{x}_P$  relative to the position of  $Q_1$  (orange). Note that

$\bar{x}_P$  moves with  $Q_1$  (orange) as  $\bar{x}_P$  is defined in terms of the relative states of the two vehicles. Because  $Q_2$  is inside the goal satisfaction BRS boundary for joining the platoon (purple dotted boundary), it is locked in to the target relative state  $\bar{x}_P$  and begins following the optimal control in Eq. (14) toward the target as long as it stays out of all safety BRSs. For example, at  $t = 5.9$ ,  $Q_2$  (purple) is outside of the safety BRS with respect to  $Q_1$  (orange), shown as the purple dashed boundary around  $Q_1$  (orange). Again, from the other safety BRS boundaries, we can see that  $Q_2$  is in fact safe with respect to all vehicles.

In the bottom plots of Fig. 8,  $Q_1$  (orange) and  $Q_2$  (purple) have already become the platoon leader and follower, respectively. The rest of the vehicles follow the same process to join the platoon. All five vehicles eventually form a single platoon and travel along the highway together. As with the first two vehicles, the goal satisfaction controllers allow the remaining vehicles to optimally and smoothly join the platoon, whereas the safety controllers prevent collisions from occurring.

## 2. Intruder Vehicle

We now consider the scenario in which a platoon of vehicles encounters an intruder vehicle. To avoid collision, each vehicle checks for safety with respect to the intruder and any vehicles in front of and behind it in the platoon. If necessary, the vehicle uses the reachability-based safety controller to avoid collision, otherwise, it

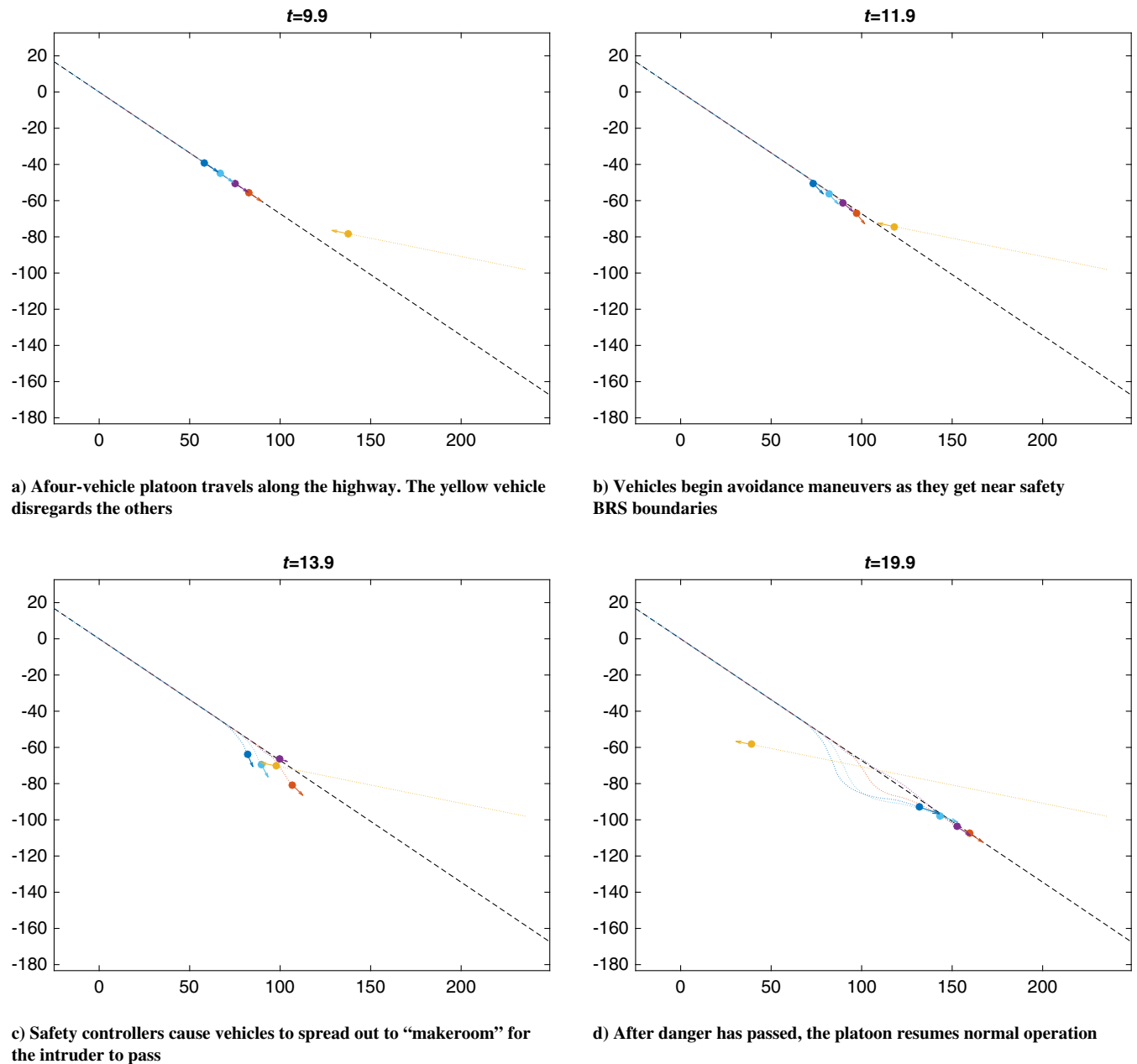


Fig. 9 Simulation showing how a platoon of four vehicles reacts to an intruder (color in online).

uses the appropriate controller to travel on the highway if it is a leader, or follow the leader if it is a follower. After danger has passed, the vehicles in the platoon resume normal operation.

Figure 9 shows the simulation result. At  $t = 9.9$ , a platoon of four vehicles  $Q_i$ ,  $i = 1, \dots, 4$  (with  $P_i = i$ ) travels along the highway shown. An intruder vehicle  $Q_5$  (yellow, the only vehicle not on the highway) heads left, disregarding the presence of the platoon. At  $t = 11.9$ , the platoon leader  $Q_1$  (red) detects that it has gone near the boundary of the safety BRS (not shown) with respect to the intruder  $Q_5$  (yellow). In response,  $Q_1$  (red) starts using the safety controller to optimally avoid the intruder according to Eq. (14); in doing so, it steers slightly off the highway.

Note that, although in this particular simulation, the intruder travels in a straight line, a straight line motion of the intruder was not assumed. Rather, the safety BRSs are computed assuming the worst-case control of the intruder, according to Eq. (14).

As the intruder  $Q_5$  (yellow) continues to disregard other vehicles, the followers of the platoon also get near the respective boundaries of their safety BRSs with respect to the intruder. This occurs at  $t = 13.9$ , where the platoon “makes room” for the intruder to pass by to avoid

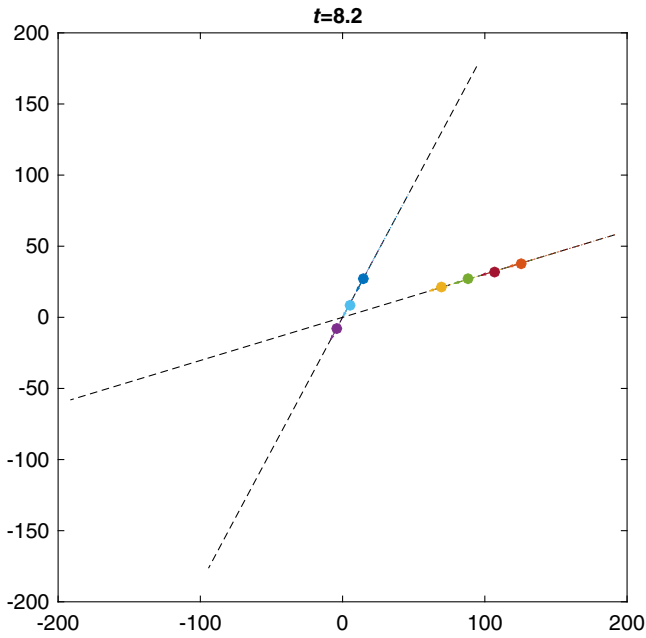
collisions; all vehicles deviate from their intended path, which is to follow the platoon leader or the highway. Note that, in this case, we have assumed that the platoon does not move as a unit in response to an intruder to show more interesting behavior.

After the intruder has passed, eventually all vehicles become far away from any safety BRSs. When this occurs, the leader resumes following the highway and the followers resume following the leader. At  $t = 19.9$ , the platoon successfully gets back onto the highway.

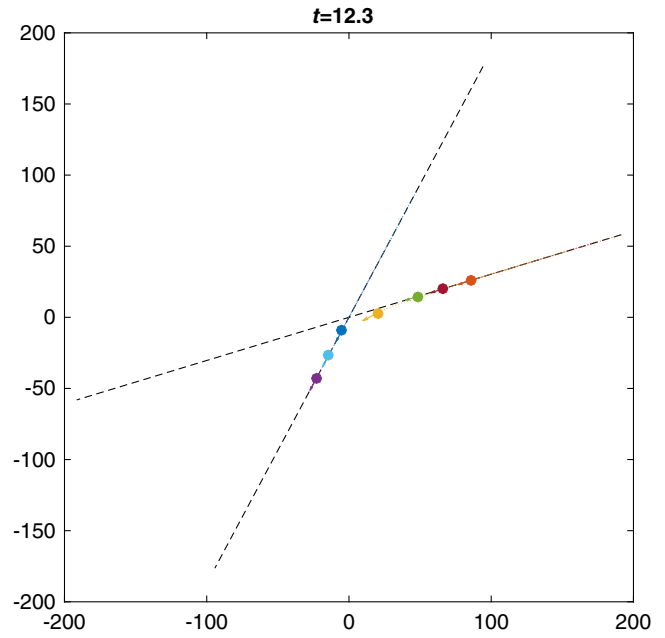
### 3. Changing Highways

To travel from origin to destination, a vehicle may need to change highways several times before exiting an air highway system. In this simulation, shown in Fig. 10, two platoons are traveling on two different highways that intersect. When the platoons are near the highway intersection, two of the vehicles in the four-vehicle platoon change highways and join the other platoon.

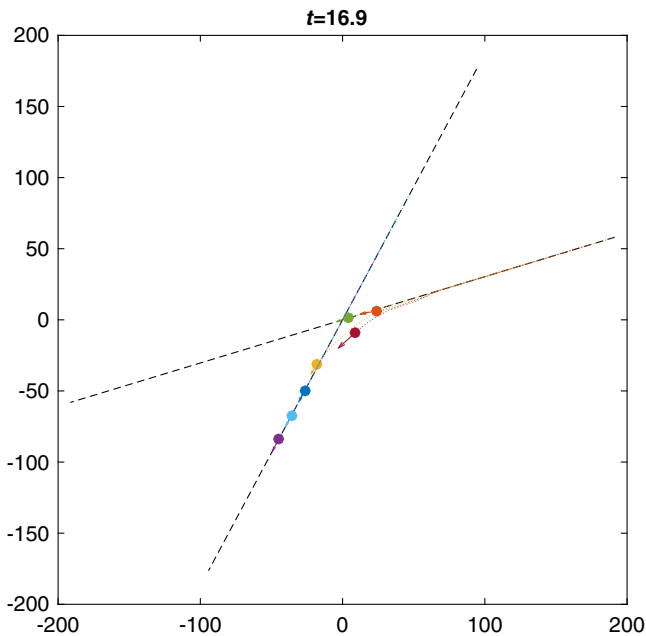
The  $t = 8.2$  plot shows the two platoons of vehicles traveling on the two air highways. One platoon has three vehicles and the other has four vehicles. At  $t = 12.3$ , the yellow vehicle (leader of the four-vehicle platoon) begins steering off its original highway to join the



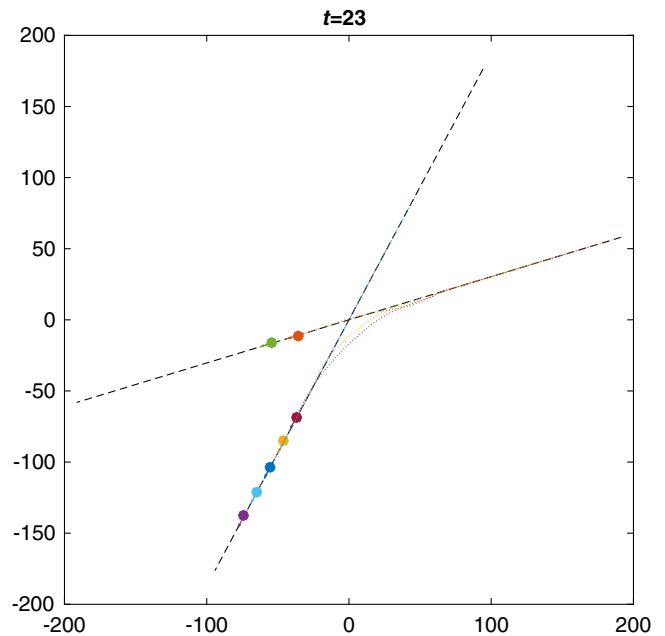
a) Three- and four-vehicle platoons travel on their respective highways



b) Yellow vehicle (leader of four-vehicle platoon) begins to join the new platoon; green vehicle (second vehicle of four-vehicle platoon) becomes a leader



c) Dark red vehicle (second vehicle of the now three-vehicle platoon) joins a new platoon; orange vehicle (last vehicle of the platoon) catches up to new platoon leader



d) New platoons now travel on their respective air highways

Fig. 10 Simulation showing two vehicles changing highways and joining a new platoon (color in online).

other platoon. In terms of the hybrid systems modes, this vehicle transitions from the leader mode to the follower mode. At the same time, the green vehicle (second vehicle of the four-vehicle platoon) transitions from the follower mode to the leader mode, because the previous platoon leader, the yellow vehicle, has left the platoon. By  $t = 16.9$ , the yellow vehicle (original leader) successfully changes highways and is now a follower in its new platoon.

At  $t = 16.9$ , the dark red vehicle is (second vehicle of the now three-vehicle platoon) in the process of changing highways. In this case, it remains in the follower mode, because it is a follower in both its old and new platoons. As this vehicle changes highways, the

orange vehicle (last vehicle of the originally four-vehicle platoon) moves forward to catch up to its new platoon leader, the green vehicle. By  $t = 23$ , all the vehicles have finished performing their desired maneuvers, resulting in a two-vehicle platoon and a five-vehicle platoon traveling on their respective highways.

#### IV. Conclusions

To address the important and urgent problem of the traffic management of UAVs, this paper has proposed to have platoons of UAVs travel on air highways. It has been shown how such an airspace



structure leads to much easier safety and goal satisfaction analysis. Simulations show that by organizing vehicles into platoons, many complex maneuvers can be performed using just a few different backward reachable sets.

For the placement of air highways over a region, the very intuitive and efficient fast marching algorithm for solving the Eikonal equation has been used. The proposed algorithm allows one to take as input any arbitrary cost map representing the desirability of flying over any position in space and produce a set of paths from any destination to a particular origin. Simple heuristic clustering methods can then be used to convert the sets of paths into a set of air highways.

On the air highways, platoons of UAVs modeled by hybrid systems were considered. It was shown how various required platoon functions (merging onto an air highway, changing platoons, etc.) can be implemented using only the free, leader, and follower modes of operation. Using HJ reachability, goal satisfaction controllers that guarantee the success of all mode transitions were proposed and a safety controller was wrapped around goal satisfaction controllers to ensure no collision between the UAVs can occur. Under the assumption that faulty vehicles can descend after a prespecified duration, the safety controller guarantees that no collisions will occur in a single altitude level as long as at most one safety breach occurs for each vehicle in the platoon. Additional safety breaches can be handled by multiple altitude ranges in the airspace.

### Acknowledgments

This work is supported in part by the National Science Foundation under Cyber-Physical Systems: ActionWebs (CNS-0931843) and Cyber-Physical Systems: Foundations Of Resilient CybEr-physical Systems (CNS1239166), by NASA under grants NNX12AR18A and UCSCMCA-14-022 (University Affiliated Research Center), by Office of Naval Research under grants N00014-12-1-0609, N000141310341 (Embedded Humans Multidisciplinary University Research Initiative), and MIT\_5710002646 (Smart Adaptive Reliable Teams for Persistent Surveillance Multidisciplinary University Research Initiative), and by Air Force Office of Scientific Research under grants UPenn-FA9550-10-1-0567 (Control of Heterogeneous Autonomous Sensors for Situational Awareness Multidisciplinary University Research Initiative) and the Science of SecUre and REsilient Cyber-Physical Systems project.

### References

- [1] Haulman, D. L., *U.S. Unmanned Aerial Vehicles in Combat, 1991–2003*, Air Force Historical Research Agency, Maxwell Air Force Base, Alabama, 2003, <http://oai.dtic.mil/oai/oai?verb=getRecord&metadataPrefix=html&>.
- [2] Stewart, J., “Google Tests Drone Deliveries in Project Wing Trials,” BBC World Service Radio, Los Angeles, 2014.
- [3] Prevot, T., Rios, J., Kopardekar, P., Robinson, J. E., III, Johnson, M., and Jung, J., “UAS Traffic Management (UTM) Concept of Operations to Safely Enable Low Altitude Flight Operations,” *Proceedings of the AIAA Aviation Technology, Integration, and Operations Conference*, AIAA Paper 2016-3292, June 2016. doi:10.2514/6.2016-3292
- [4] DeBusk, W., “Unmanned Aerial Vehicle Systems for Disaster Relief: Tornado Alley,” *AIAA Infotech@Aerospace 2010*, AIAA Paper 2010-3506, April 2010. doi:10.2514/6.2010-3506
- [5] “UAS Aid in South Carolina Tornado Investigation,” AUVSI News [online], Assoc. for Unmanned Vehicle Systems International, Arlington, VA, Jan. 2016, <http://www.auvsi.org/blogs/auvsi-news/2016/01/29/tornado> [retrieved 16 Feb. 2016].
- [6] “Unmanned Aircraft Systems (UAS) Comprehensive Plan—A Report on the Nation’s UAS Path Forward,” Jointed Planning, and Development Office, Federal Aviation Administration, Technical Rept., 2013.
- [7] “Challenge is on to Design Sky for All,” NASA, Dec. 2015, <http://www.nasa.gov/feature/challenge-is-on-to-design-sky-for-all> [retrieved 12 Feb. 2016].
- [8] Bokanowski, O., Forcadel, N., and Zidani, H., “Reachability and Minimal Times for State Constrained Nonlinear Problems Without Any

- Controllability Assumption,” *SIAM Journal on Control and Optimization*, Vol. 48, No. 7, Jan. 2010, pp. 4292–4316. doi:10.1137/090762075
- [9] Mitchell, I. M., Bayen, A. M., and Tomlin, C. J., “A Time-Dependent Hamilton–Jacobi Formulation of Reachable Sets for Continuous Dynamic Games,” *IEEE Transactions on Automatic Control*, Vol. 50, No. 7, July 2005, pp. 947–957.
- [10] Barron, E., and Ishii, H., “The Bellman Equation for Minimizing the Maximum Cost,” *Nonlinear Analysis: Theory, Methods & Applications*, Vol. 13, No. 9, Sept. 1989, pp. 1067–1090. doi:10.1016/0362-546X(89)90096-5
- [11] Fisac, J. F., Chen, M., Tomlin, C. J., and Sastry, S. S., “Reach-Avoid Problems with Time-Varying Dynamics, Targets and Constraints,” *Proceedings of the International Conference on Hybrid Systems: Computation and Control*, Association for Computing Machinery, 2015, pp. 11–20. doi:10.1145/2728606.2728612
- [12] Chen, M., Zhou, Z., and Tomlin, C. J., “Multiplayer Reach-Avoid Games via Low Dimensional Solutions and Maximum Matching,” *Proceedings of the American Control Conference*, IEEE Publ., Piscataway, NJ, 2014, pp. 1444–1449. doi:10.1109/ACC.2014.6859219
- [13] Chen, M., Zhou, Z., and Tomlin, C. J., “Multiplayer Reach-Avoid Games via Pairwise Outcomes,” *IEEE Transactions on Automatic Control*, Vol. PP, No. 99, 2016, p. 1. doi:10.1109/TAC.2016.2577619
- [14] Ding, J., Sprinkle, J., Sastry, S. S., and Tomlin, C. J., “Reachability Calculations for Automated Aerial Refueling,” *Proceedings of the IEEE Conference on Decision and Control*, IEEE Publ., Piscataway, NJ, 2008, pp. 3706–3712. doi:10.1109/CDC.2008.4738998
- [15] Mitchell, I. M., “The Flexible, Extensible and Efficient Toolbox of Level Set Methods,” *Journal of Scientific Computing*, Vol. 35, Nos. 2–3, June 2008, pp. 300–329. doi:10.1007/s10915-007-9174-4
- [16] Osher, S., and Fedkiw, R., *Level Set Methods and Dynamic Implicit Surfaces*, Springer–Verlag, Berlin, 2002.
- [17] Sethian, J. A., “A Fast Marching Level Set Method for Monotonically Advancing Fronts,” *Proceedings of the National Academy of Sciences*, Vol. 93, No. 4, Feb. 1996, pp. 1591–1595. doi:10.1073/pnas.93.4.1591
- [18] Kavathekar, P., and Chen, Y., “Vehicle Platooning: A Brief Survey and Categorization,” *Proceedings of the ASME/IEEE International Conference on Mechatronic and Embedded Systems and Applications, Parts A and B*, Vol. 3, American Soc. of Mechanical Engineers, New York, 2011, pp. 829–845. doi:10.1115/DETC2011-47861
- [19] McMahon, H. D., Hedrick, K. J., and Shladover, E. S., “Vehicle Modelling and Control for Automated Highway Systems,” *American Control Conference*, IEEE Publ., Piscataway, NJ, May 1990, pp. 297–303.
- [20] Hedrick, K. J., Zhang, G., Narendran, K. V., and Chang, K. S., *Transitional Platoon Maneuvers in an Automated Highway System*, Inst. of Transportation Studies, Univ. of California, Berkeley, CA, 1992.
- [21] Lygeros, J., Godbole, D. N., and Sastry, S. S., “Verified Hybrid Controllers for Automated Vehicles,” *IEEE Transactions on Automatic Control*, Vol. 43, No. 4, April 1998, pp. 522–539.
- [22] Gattami, A., Al Alam, A., Johansson, K. H., and Tomlin, C. J., “Establishing Safety for Heavy Duty Vehicle Platooning: A Game Theoretical Approach,” *IFAC Proceedings*, Vol. 44, No. 1, Jan. 2011, pp. 3818–3823. doi:10.3182/20110828-6-IT-1002.02071
- [23] Sabau, S., Oara, C., Warnick, S., and Jadbabaie, A., “Optimal Distributed Control for Platooning via Sparse Coprime Factorizations,” *IEEE Transactions on Automatic Control*, Vol. 62, No. 1, 2016, p. 1. doi:10.1109/TAC.2016.2572002
- [24] Crandall, M. G., Evans, L. C., and Lions, P.-L., “Some Properties of Viscosity Solutions of Hamilton–Jacobi Equations,” *Transactions of the American Mathematical Society*, Vol. 282, No. 2, April 1984, pp. 487–502. doi:S0002-9947-1984-0732102-X
- [25] Alton, K., and Mitchell, I., “Optimal Path Planning Under Different Norms in Continuous State Spaces,” *Proceedings of the IEEE International Conference on Robotics and Automation*, IEEE Publ., Piscataway, NJ, 2006, pp. 866–872. doi:10.1109/ROBOT.2006.1641818
- [26] Lygeros, J., Sastry, S., and Tomlin, C., *Hybrid Systems: Foundations, Advanced Topics and Applications*, Springer–Verlag, New York, 2012.
- [27] Adler, A., Bar-Gill, A., and Shimkin, N., “Optimal Flight Paths for Engine-Out Emergency Landing,” *Proceedings of the IEEE Chinese*

- Control and Decision Conference*, IEEE Publ., Piscataway, NJ, 2012, pp. 2908–2915.  
doi:10.1109/CCDC.2012.6244461
- [28] Coombes, M., Chen, W.-H., and Render, P., “Reachability Analysis of Landing Sites for Forced Landing of a UAS,” *Journal of Intelligent & Robotic Systems*, Vol. 73, Nos. 1–4, Jan. 2014, pp. 635–653.  
doi:10.1007/s10846-013-9920-9
- [29] Idicula, J., Akametalu, K., Chen, M., Tomlin, C., Ding, J., and Hook, L., “Where to Land: A Reachability Based Forced Landing Algorithm for Aircraft Engine Out Scenarios,” *Seedling Technical Seminar*, NASA Dryden Flight Research Center, Rept. DFRC-E-DAA-TN28194, Nov. 2015.
- [30] Evans, L. C., and Souganidis, P. E., “Differential Games and Representation Formulas for Solutions of Hamilton–Jacobi–Isaacs Equations,” *Indiana University Mathematics Journal*, Vol. 33, No. 5, 1984, pp. 773–797.
- [31] Varaiya, P. P., “On the Existence of Solutions to a Differential Game,” *SIAM Journal on Control*, Vol. 5, No. 1, Feb. 1967, pp. 153–162.  
doi:10.1137/0305009
- [32] Chen, M., and Tomlin, C. J., “Exact and Efficient Hamilton–Jacobi Reachability for Decoupled Systems,” *Proceedings of the IEEE Conference on Decision and Control*, IEEE Publ., Piscataway, NJ, 2015, pp. 1297–1303.  
doi:10.1109/CDC.2015.7402390
- [33] Chen, M., Herbert, S., and Tomlin, C. J., “Exact and Efficient Hamilton–Jacobi-based Guaranteed Safety Analysis via System Decomposition,” *IEEE International Conference on Robotics and Automation* (submitted for publication).
- [34] Chen, M., Herbert, S., Vashishtha, M., Bansal, S., and Tomlin, C. J., “A General System Decomposition Method for Computing Reachable Sets and Tubes,” *IEEE Transactions on Automatic Control* (submitted for publication).
- [35] Bansal, S., Chen, M., and Tomlin, C. J., “Safe Sequential Path Planning of Multi-Vehicle Systems Under Presence of Disturbances and Measurement Noise,” *American Control Conference* (submitted for publication).
- [36] Chen, M., Shih, J., and Tomlin, C. J., “Multi-Vehicle Collision Avoidance via Reachability and Mixed Integer Programming,” *Proceedings of the IEEE Conference on Decision and Control* (to be published).

This article has been cited by:

1. Alena Otto, Niels Agatz, James Campbell, Bruce Golden, Erwin Pesch. 2018. Optimization approaches for civil applications of unmanned aerial vehicles (UAVs) or aerial drones: A survey. *Networks* **72**:4, 411–458. [[Crossref](#)]
2. Mo Chen, Claire J. Tomlin. 2018. Hamilton–Jacobi Reachability: Some Recent Theoretical Advances and Applications in Unmanned Airspace Management. *Annual Review of Control, Robotics, and Autonomous Systems* **1**:1, 333–358. [[Crossref](#)]
3. Ping Liu, Guodong Li, Xinggao Liu, Long Xiao, Yalin Wang, Chunhua Yang, Weihua Gui. 2018. A novel non-uniform control vector parameterization approach with time grid refinement for flight level tracking optimal control problems. *ISA Transactions* **73**, 66–78. [[Crossref](#)]
4. Edward A. Lee, Marjan Sirjani. What Good are Models? 3–31. [[Crossref](#)]
5. Aparna Dhinakaran, Mo Chen, Glen Chou, Jennifer C. Shih, Claire J. Tomlin. A hybrid framework for multi-vehicle collision avoidance 2979–2984. [[Crossref](#)]
6. Somil Bansal, Mo Chen, Sylvia Herbert, Claire J. Tomlin. Hamilton–Jacobi reachability: A brief overview and recent advances 2242–2253. [[Crossref](#)]